

pH-Responsive Biohybrid Carrier Material for Phenol Decontamination in Wastewater

Martin Pretscher,^{†,‡} Beatriz A. Pineda-Contreras,^{†,‡} Patrick Kaiser,[§] Steffen Reich,[†] Judith Schöbel,[†] Christian Kuttner,^{||,&ID} Ruth Freitag,^{§,ID} Andreas Fery,^{||} Holger Schmalz,^{†,⊥} and Seema Agarwal^{*,†,‡,#ID}

[†]Macromolecular Chemistry II, University of Bayreuth, Universitätsstraße 30, 95440, Bayreuth, Germany

[§]Process Biotechnology, University of Bayreuth, Universitätsstraße 30, 95440 Bayreuth, Germany

^{||}Leibniz Institute of Polymer Research Dresden, Institute of Physical Chemistry and Polymer Physics, Hohe Straße 6, 01069 Dresden, Germany

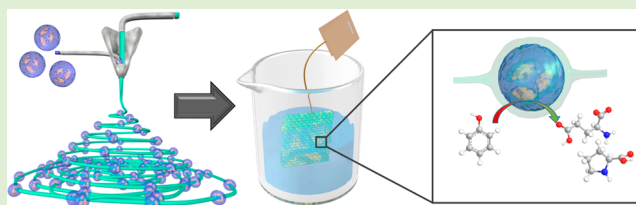
[&]BioNanoPlasmonics Laboratory, CIC biomaGUNE, Paseo de Miramón 182, 20014 Donostia-San Sebastián, Spain

[⊥]Bavarian Polymer Institute, University of Bayreuth, Universitätsstraße 30, 95440, Bayreuth, Germany

[#]Bayreuth Center for Colloids and Interfaces, University of Bayreuth, Universitätsstraße 30, 95440, Bayreuth, Germany

Supporting Information

ABSTRACT: Smart polymers are a valuable platform to protect and control the activity of biological agents over a wide range of conditions, such as low pH, by proper encapsulation. Such conditions are present in olive oil mill wastewater with phenol as one of the most problematic constituents. We show that elastic and pH-responsive diblock copolymer fibers are a suitable carrier for *Corynebacterium glutamicum*, i.e., bacteria which are known for their ability to degrade phenol. Free *C. glutamicum* does not survive low pH conditions and fails to degrade phenol at low pH conditions. Our tea-bag like biohybrid system, where the pH-responsive diblock copolymer acts as a protecting outer shell for the embedded bacteria, allows phenol degradation even at low pH. Utilizing a two-step encapsulation process, planktonic cells were first encapsulated in poly(vinyl alcohol) to protect the bacteria against the organic solvents used in the second step employing coaxial electrospinning.



INTRODUCTION

Water is one of the most important natural resources on our planet. Therefore, there have been increasing efforts to improve the treatment of wastewater, which is generated in large amounts by different industries, including the olive oil industry.^{1–4} In each case toxic organic compounds, e.g., phenol, polyphenols, and further derivatives, are present in the olive oil mill wastewater (OMW).^{5–7} The application of chemical methods to approach the treatment of OMW are associated with high costs and further addition of toxic compounds.^{2,8} Thus, biological wastewater treatment has been proposed as an environmentally compatible and cost-effective alternative in view of the significant disadvantages of chemical treatments. In this respect, several bacterial and fungal species, such as *Alcaligenes eutrophus*,⁹ *Acinetobacter calcoaceticus*,¹⁰ *Pseudomonas* genus,² *Phanerochaete chrysosporium*,¹¹ etc., have revealed capability for the biodegradation of organic pollutants like phenol.² A significant variety of these microorganisms can be isolated from contaminated wastewater.^{12–14} *C. glutamicum* is a Gram-positive bacterium with tolerance to phenol and showing a high activity in the degradation of aromatic compounds.^{15,16} The use of immobilized bacteria for phenol degradation presents the opportunity of a reusable biological

system,¹⁷ avoiding further contamination of wastewater with free microbes.

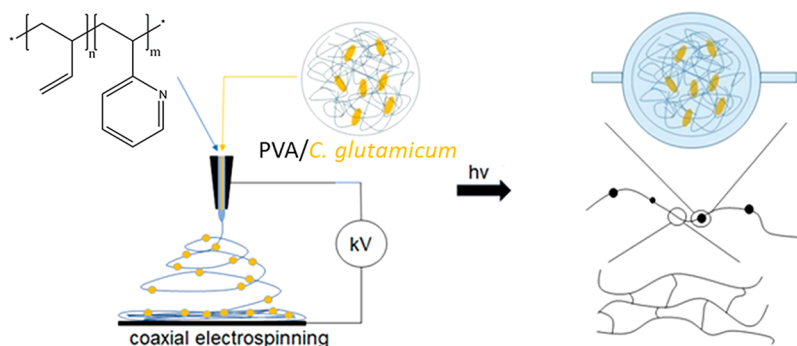
Electrospinning has been extensively used for the immobilization of bioactive agents in nanofibers, due to its easy handling and high versatility. In this context, coaxial electrospinning is an alternative technique to the conventional electrospinning process, often used to maintain the viability of active agents such as bacteria.¹⁸ Gensheimer et al. confirmed the survival under dry storage conditions of *Escherichia coli* and *Micrococcus luteus* embedded in cross-linked poly(vinyl alcohol) (PVA) particles, used in further electrospinning encapsulation.¹⁹ Knierim et al. showed that biological agents are accessible for waste separation in electrospun nonwovens.²⁰ “Living composites” with *Candida tropicalis* yeast, formed via coaxial electrospinning, showed a phenol degradation of 60% after treatment in OMW for 72 h.²¹ Nardi and co-workers carried out investigations on biodegradation of OMW using immobilized *C. glutamicum* in electrospun fibers.²² They compared the phenol degradation capacity of free and encapsulated bacteria, describing the importance of mass

Received: March 1, 2018

Revised: May 2, 2018

Published: June 25, 2018

Scheme 1. Preparation of pH-Responsive Biohybrid Carrier Materials for Phenol Degradation via Coaxial Electrospinning of Bacteria Loaded PVA Particles (Core) and a pH-Responsive PB-*b*-P2VP Diblock Copolymer (Shell), Followed by UV Cross-Linking



transport as well as the influence of the produced metabolized products in the immobilized system. However, there is still a need for systematic studies, as quantifications regarding bacteria concentration, amount of employed nonwoven for decontamination and aging effects are missing.

Next to the successful immobilization of bacteria, like *C. glutamicum*, within electrospun nonwovens an important issue is to provide a suitable microenvironment to ensure a sufficient stability of the nonwoven (high reusability, no leakage of bacteria over time) and most importantly the viability of the bacteria. This is especially relevant in OMW detoxification, as its low pH is toxic to many bacteria including *C. glutamicum*. A possible solution to these problems might be the use of diblock copolymers as shell material that provide a pH-responsive block, protecting the bacteria from the low pH of OMW by acting as a buffer, and an elastic block, providing the necessary mechanical stability and flexibility to the electrospun nonwoven. Accordingly, diblock copolymers of polybutadiene and poly(2-vinylpyridine) (PB-*b*-P2VP) could be considered as a possible biocarrier system for application in wastewater treatment. In these diblock copolymers, the pH-responsivity of P2VP at acidic conditions, which makes it suitable for applications in acidic media such as OMW, is combined with the low glass transition temperature of the PB block, offering a flexible and mechanically stable matrix after cross-linking to support a suitable microenvironment for the immobilized cells. Here, the block-type structure is indispensable, as for a random copolymer the necessary low glass transition of the soft phase cannot be realized.

In this work, we present a two-step encapsulation process to prepare a pH-responsive biohybrid carrier material for phenol degradation in OMW even at low pH (Scheme 1). In the first step, *C. glutamicum* is encapsulated in PVA particles to allow electrospinning of the bacteria from otherwise toxic organic solvents. Subsequently, using a coaxial electrospinning setup with the bacteria loaded PVA dispersion as core and the PB-*b*-P2VP diblock copolymer solution as shell gives access to the desired pH-responsive nonwovens after subsequent UV cross-linking. This tea bag-like system is then successfully employed in phenol degradation even at pH = 4, which is not possible with nonimmobilized *C. glutamicum*.

EXPERIMENTAL SECTION

Materials. THF (Sigma-Aldrich, p.a.) was distilled from CaH₂ and potassium and kept under dry nitrogen until use. *Sec*-butyllithium (*sec*-BuLi, Acros, 1.3 M in cyclohexane/hexane: 92/8) was used without further purification. Butadiene (Riessner-Gase) was passed

over columns filled with molecular sieves and basic aluminum oxide. Subsequently, butadiene was condensed in a glass reactor and stored over dibutylmagnesium. 2-Vinylpyridine (2VP, Sigma-Aldrich, 97%) was degassed and dried over triethylaluminum (Et₃Al, 1 M, Sigma-Aldrich) for 2 h. Subsequently, the calculated amount of monomer was condensed on a high vacuum line into a glass ampule and stored under nitrogen until use. 1,1-Diphenylethylene (DPE) was distilled from *sec*-BuLi under reduced pressure. Photo initiators: ethyl 4-(dimethylamino)benzoate (EDMAB, 99%) and camphorquinone (CQ, 97%) were supplied by Sigma-Aldrich and used without further purification. For bacteria encapsulation in PVA particles: *C. glutamicum* (DSM-No. 20300, DSMZ Braunschweig), LB-medium (Lennox, Roth), PVA (Kuraray Specialties Europa, $M_w = 145\,000\text{ g mol}^{-1}$, 98–99 mol % hydrolysis) and silicone oil (AP200, Wacker) were used. Technical grade acetone was distilled prior to use. Phenol (BioUltra, for molecular biology, ≥99.5% (GC)) was obtained from Sigma-Aldrich and stored under sterile conditions.

Synthesis of the PB-*b*-P2VP Diblock Copolymer. The synthesis of the PB-*b*-P2VP diblock copolymer was carried out via sequential living anionic polymerization in THF employing a thermostated laboratory autoclave (Büchi AG). After cooling to $-70\text{ }^\circ\text{C}$, *sec*-BuLi was added as initiator for the butadiene polymerization. Subsequently, butadiene was added and the polymerization was conducted at $-10\text{ }^\circ\text{C}$ for 8 h. A small aliquot of the solution was precipitated from degassed methanol for MALDI-TOF and SEC analysis. The reaction mixture was cooled to $-70\text{ }^\circ\text{C}$ and DPE (1.1 equiv with respect to *sec*-BuLi) was added. After stirring for 15 min, 2VP was added and reacted for 2.5 h. The reaction was terminated by adding 1 mL of degassed methanol. The polymer was precipitated from deionized water, filtered, and freeze-dried from 1,4-dioxane. Further details about the synthesis and analysis of the obtained B₆₆V₃₄¹²⁶ diblock copolymer (subscripts denote the mass fraction of the respective block and the superscript gives the overall number-averaged molecular weight M_n in kg mol⁻¹) can be found in the Supporting Information.

Formation of Nanofibers by Electrospinning. For electrospinning of monolithic fibers, a 15 wt % solution of B₆₆V₃₄¹²⁶ in a mixture of THF/DMF (80/20, v/v) was prepared. In this case, the conventional one needle setup was used for electrospinning at high voltage (16 kV). The fibers were collected on a stainless steel mesh at a flow rate of 1000 μL min⁻¹. For bacteria encapsulation, coaxial electrospinning was required. Two separated solutions were prepared, the outer shell was formed using the same polymer solution as for the monolithic fibers at the same flow rate. The core was made of a suspension of PVA/bacteria particles in THF (10 g L⁻¹), employing a flow rate of 750 μL min⁻¹. The nanofiber nonwoven was collected on a sterile stainless steel mesh and subsequently cross-linked using a commercial blue light LED source (2.01 mW cm⁻² at λ = 465 nm), employing exposure times of 15 min. A cross-linking system containing an equimolar mixture of CQ and EDMAB in 20 wt % concentration with respect to the amount of polymer was directly

dissolved with the polymer in the THF/DMF mixture used for electrospinning.

Culture Conditions of Planktonic Cells and Preparation of *C. glutamicum* Loaded PVA Particles. The nutrient media was prepared by dissolving 1.6 g of LB-media powder in 80 mL of deionized water. This solution was sterilized in an autoclave at 121 °C. After cooling down, one colony of *C. glutamicum* was transferred with an inoculation loop to the nutrient solution. *C. glutamicum* was grown by incubation of the nutrient bacteria solution at 30 °C for 24 h in a shaker at 150 rpm. The bacteria pellet was centrifuged at 4000 rpm for 10 min and subsequently washed three times with sterile phosphate buffer solution.

Immobilization of *C. glutamicum* in PVA Particles. A 10 wt % aqueous PVA solution was sterilized with an autoclave at 121 °C. The silicone oil was sterilized with a sterile syringe filter with a mesh size of 0.20 μm . The PVA/*C. glutamicum* particles were prepared by dispersing $7.0\text{--}7.5 \times 10^8$ CFU in 10 mL of the aqueous PVA solution ($c = 10$ wt %). Five mL of the bacteria dispersion were immersed in 80 mL silicone oil and redispersed with an ultra turrax disperser (IKA) with an 18G dispersing tool at 10000 rpm for 10 min. The obtained dispersion was added directly to 300 mL acetone and stirred for 30 min. PVA/*C. glutamicum* particles were obtained by centrifugation at 4000 rpm (4 °C) for 10 min. The mean diameter of the PVA/*C. glutamicum* particles was $5.9 \pm 3.1 \mu\text{m}$. The particle size was calculated by measuring 140 particles with ImageJ. The dry particles with theoretically $3.5\text{--}3.7 \times 10^8$ CFU in 500 mg were stored at 4 °C for further use.

Culture of Planktonic and Encapsulated Bacteria with Basal Media. The planktonic and encapsulated (in PVA particles or nonwovens) bacteria were cultivated in sealed shake flasks (250 mL) containing 100 mL *C. glutamicum* basal media (BMCG), supplemented with 0.4 g L^{-1} phenol and without phenol (control), respectively. The pH of the media was regulated in the range from 4 to 7 as described by Liebl et al.²³ The growth media was prepared with following composition (per liter): 7 g of $(\text{NH}_4)_2\text{SO}_4$, 6 g of Na_2HPO_4 , 3 g of KH_2PO_4 , 0.5 g of NaCl, 1 g of NH_4Cl . The required pH was adjusted with 2 M NaOH and H_3PO_4 (85%). After autoclaving at 121 °C for 20 min, the media was supplemented with 5 mL of salt stock (containing 8 g of $\text{MgSO}_4 \cdot 7 \text{H}_2\text{O}$, 4 g of $\text{FeSO}_4 \cdot 7 \text{H}_2\text{O}$, 0.04 g of $\text{MnSO}_4 \cdot \text{H}_2\text{O}$, and 0.5 g of NaCl), 2 mL of mineral mix (containing 0.088 g of $\text{Na}_2\text{B}_4\text{O}_7 \cdot 10 \text{H}_2\text{O}$, 0.04 g of $(\text{NH}_4)_6\text{Mo}_7\text{O}_{24} \cdot 4 \text{H}_2\text{O}$, 0.01 g of $\text{ZnSO}_4 \cdot 7 \text{H}_2\text{O}$, 0.172 g of CuSO_4 , 0.0072 g $\text{MnCl}_2 \cdot 4 \text{H}_2\text{O}$, 0.87 g of $\text{FeCl}_3 \cdot 6 \text{H}_2\text{O}$, sterile filtered), 0.05 mL of calcium chloride stock (148.9 g L^{-1} , autoclaved), 1 mL of vitamin stock (1 g L^{-1} biotin and 10 g L^{-1} thiamine hydrochloride, sterile filtered) as well as 50 mL of glucose stock (220 g L^{-1} , autoclaved). For cultivating planktonic *C. glutamicum*, the shake flasks containing BMCG media with different pH values were inoculated with an optical density at $\lambda = 600$ nm (OD_{600}) of 1.5 from an overnight culture and shook at 150 rpm at 30 °C for 142 h. The PVA/bacteria particles and nonwovens were cultivated at 30 °C and 25 rpm at different pH values as described above. Every 24 h, samples were taken under sterile conditions and in case of the planktonic cultures the OD_{600} was determined. To detect planktonic cells, 100 μL of the media was seeded on LB agar plates and incubated at 30 °C for 72 h.

Analytical Techniques. ^1H NMR measurements were performed on a 300 MHz Bruker Ultrashield 300 spectrometer using $\text{THF-}d_8$ as solvent.

For MALDI-TOF, a Bruker Reflex III equipped with a N_2 laser ($\lambda = 337$ nm) was used in linear mode at an acceleration voltage of 20 kV. The sample preparation was done according to the dried-droplet method. Therefore, matrix (trans-2-[3-(4-*tert*-butylphenyl)-2-methyl-2-propenylidene]malononitrile (DCTB), 20 g L^{-1}), analyte (10 g L^{-1}), and salt (silver trifluoroacetate, 10 g L^{-1}) were dissolved and mixed in THF in the ratio of 20:5:1 and 0.5 μL were spotted onto the target plate.

Size exclusion chromatography (SEC) was carried out with THF as eluent at a flow rate of 1.0 mL min^{-1} to determine the apparent molecular weights and molecular weight distributions of the polymers, respectively. Two PLGel mixed-D columns (particle size 5 μm ,

dimension 7.5 mm \times 300 mm) calibrated with narrowly distributed polystyrene standards were employed together with a refractive index detector RI 101 from Shodex. SEC data were analyzed using the software WinGpc7.

Swelling and deswelling of PB-*b*-P2VP diblock copolymer films at different pH values (pH = 2–8) were studied by *in situ* spectroscopic ellipsometry (Supporting Information). To this end, thin films were prepared by spin-casting a 2 wt % polymer solution in THF onto silicon wafers. A commercial polarizer-compensator-sample-analyzer (PCSA) configuration (SE800, Sentech) with a xenon lamp as white-light source was used. Measurements in liquid were performed using a self-built flow cell. For switching between different pH values, the *in situ* cell was purged twice with deionized water to remove the old buffer solution. Afterward, the cell was filled with new pH buffer, purged, and filled again with the new pH buffer solution. At each new pH, equilibration of the sample was reached after 20 min.

Atomic force microscopy (AFM) measurements on thin diblock copolymer films, formed via spin-casting from THF, were carried out at room temperature with a commercial AFM Dimension Icon by Bruker. In all images, the color scale was set for maximum visibility. All micrographs were measured at 512×512 pixel² resolution.

The morphology of PB-*b*-P2VP diblock copolymer films and electrospun fibers was observed by transmission electron microscopy (TEM), employing a Zeiss CEM902 electron microscope operated at an acceleration voltage of 80 kV. Zero-loss filtered images were registered digitally by a side mounted CCD camera system (Orius SC200W, Gatan) and processed with a digital imaging processing system (Gatan Digital Micrograph 2.3, Gatan). The films were prepared by solvent casting of a 1 wt % solution of the diblock copolymer in THF. Microtome cutting of the films as well as the electrospun fibers was performed on a Leica EM FC7 ultramicrotome well below the glass transition temperature of PB. Therefore, the samples were prepared onto adhesive tape and cooled to -160 °C in DMSO. For cutting, the knife was cooled to -30 °C. Samples with a thickness of 50–60 nm were obtained and prepared onto copper grids. The PB domains were selectively stained by exposing the sample to OsO_4 vapor for 1 min at a reduced pressure of 200 mbar.

Film and fiber surface morphologies were observed with a scanning electron microscope (SEM, Zeiss LEO 1530), operating at an acceleration voltage of 3 kV employing an Everhart-Thornley secondary electron detector. Prior imaging, the samples were sputter-coated (Sputter Coater 208HR) with a thin platinum layer of 2.0 nm.

Tensile tests were carried out using a Zwick/Roell BT1-FR 0.5TN-D14 equipment. For sample testing, a 200 N KAF-TC load sensor was used with a strain rate of 25 mm min^{-1} and a preload of 0.02 N mm^{-1} at 21 °C. Test samples were formed into dog bone shape (length 30 mm and width 2 mm) using a Ray-Ran cutting press equipment. Data analysis was carried out with the Zwick Roell testXpert II V 3.0 software. The tensile moduli were determined from the slope of the stress–strain-curves. The tensile strength was defined as the maximum point of the stress–strain curves using an average of four samples.

For confocal Raman imaging a WITec alpha 300 RA+ imaging system equipment with a UHTS 300 spectrometer and a back-illuminated Andor Newton 970 EMCCD camera was used. The measurements were conducted employing an excitation wavelength of $\lambda = 532$ nm and an integration time of 0.5 s pixel⁻¹ (100 \times objective, NA = 0.9, step size 100 nm, software WITec Control FOUR 4.1). All spectra were subjected to a cosmic ray removal routine and baseline correction. The spatial distribution of PVA and *C. glutamicum* in the particles was determined by basis analysis using the Raman spectra of the neat components as references (software WITec Project FOUR 4.1).

Phenol degradation was followed by gas chromatography coupled with mass spectrometry (GC-MS, Agilent 5977A MSD), using helium as carrier gas and a HP-5MS 30 m \times 0.250 mm column. The injector temperature was 300 °C. Phenol containing samples were taken regularly under sterile conditions and frozen at -30 °C until analysis was carried out. For analysis, 200 μL of the aqueous sample was

extracted with ethyl acetate (2 mL) with an internal standard of undecane and measured afterward. To determine the phenol concentration, the solution at $t = 0$ was used as reference.

RESULTS AND DISCUSSION

Electrospinning of pH-Responsive Monolithic PB-*b*-P2VP Fibers. The pH-responsive PB-*b*-P2VP diblock copolymer ($B_{66}V_{34}^{126}$), where the subscripts denote the mass fraction of the respective block and the superscript gives the overall number-averaged molecular weight M_n in kg mol^{-1} , was prepared by sequential anionic polymerization, as described elsewhere.²⁴ The 1,2-PB precursor (87% 1,2-addition) as well as the diblock copolymer exhibited narrow molecular weight distributions ($\bar{D} = 1.01$). A detailed characterization of the $B_{66}V_{34}^{126}$ diblock copolymer can be found in the Supporting Information (Figure S1).

Fibers of the $B_{66}V_{34}^{126}$ diblock copolymer were fabricated by electrospinning using a one needle setup. Due to the low glass transition temperature of the PB block ($T_g = -3\text{ }^\circ\text{C}$) it was necessary to cross-link the obtained fibers to improve the stability and avoid film formation. Figure 1A shows the SEM

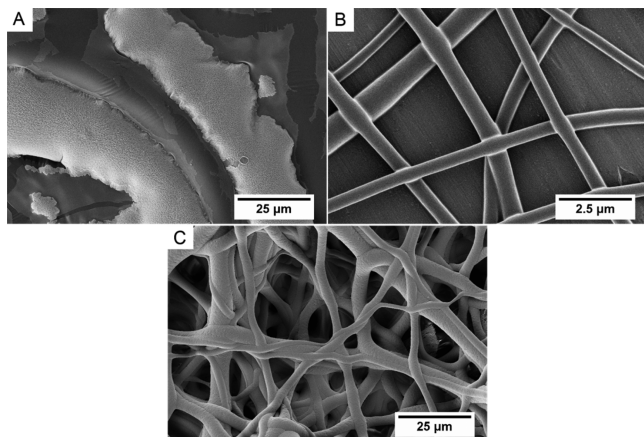


Figure 1. SEM images of electrospun $B_{66}V_{34}^{126}$ fibers. (A) Non-cross-linked fibers showing film formation. (B) Cross-linked fibers with a cross-linking system containing an equimolar CQ/EDMAB mixture (20 wt %). (C) Cross-linked fibers after treatment at $\text{pH} = 2$ over 6 days.

image of electrospun PB-*b*-P2VP fibers without cross-linking. Due to the low T_g of PB these fibers lost their shape and formed a polymeric film. In contrast, photo cross-linked electrospun fibers kept their fiber morphology in the dry state after storage for 10 days (Figure 1B) and even remained stable after treatment with acidic water of $\text{pH} = 2$ for 6 days. The stability at low pH , where the 2-vinylpyridine units are protonated, is very important, since the application of these electrospun fibers for phenol degradation is assigned to an acidic environment. Mechanical testing of the nonwovens showed a high effective Young's modulus of $E = 20\text{ MPa}$ with an elongation at break in the range of 100–200%, which are close to the values observed for cross-linked $B_{66}V_{34}^{126}$ diblock copolymer films (Figure S2).

The morphology of the $B_{66}V_{34}^{126}$ diblock copolymer was studied on films prepared by slow solution casting from THF. For TEM measurements the PB block was selectively stained with OsO_4 , which consequently appears dark in the TEM micrographs. According to the composition of the diblock copolymer the TEM micrograph in Figure 2A shows closely

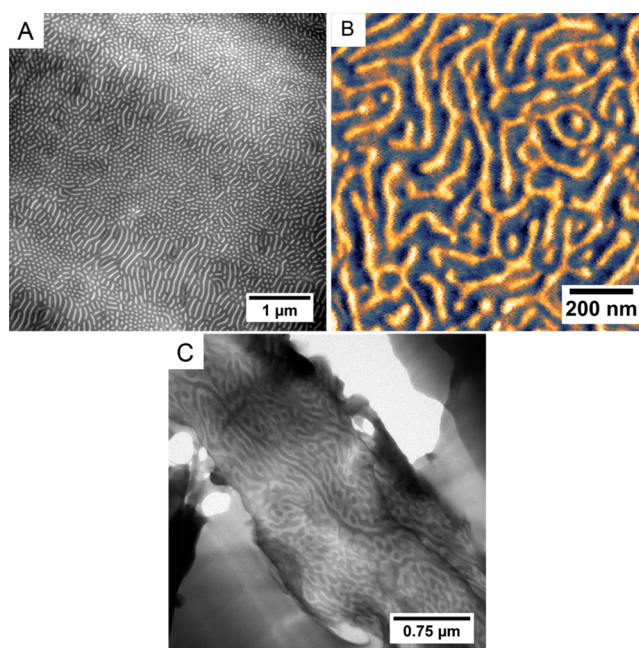


Figure 2. (A) TEM micrograph of a $B_{66}V_{34}^{126}$ film formed via slow casting from THF (PB selectively stained with OsO_4). (B) AFM phase image of a $B_{66}V_{34}^{126}$ film scaled for maximum visibility. (C) TEM micrograph of a thin section of a cross-linked electrospun $B_{66}V_{34}^{126}$ fiber, showing microphase separation (PB selectively stained with OsO_4).

packed P2VP cylinders (appear bright) embedded in a PB matrix (appears dark). For samples casted via spin coating, cylindrical structures were observed as well by AFM but were less aligned due to the fast evaporation of the solvent (Figure 2B).²⁶ These less aligned cylindrical structures can also be observed for the electrospun $B_{66}V_{34}^{126}$ fibers (Figure 2C).

The $B_{66}V_{34}^{126}$ diblock copolymer shows pH-responsive behavior due to the protonation of the pyridine units in the P2VP block ($\text{p}K_a = 4.9$).^{25,26} At neutral or higher pH , deprotonation occurs and the P2VP block becomes hydrophobic. To study the pH-responsive behavior of the diblock copolymer, we prepared thin films by spin-casting from THF solution onto a silicon wafer with later cross-linking as a model system, since quantification of the swelling/deswelling behavior of electrospun fibers was difficult. In order to monitor the swelling behavior, the optical properties of the polymer need to be quantified. For this purpose, the film thickness in the dry state determined by AFM ($d = 130 \pm 5\text{ nm}$) served as a reference value for the spectroscopic ellipsometry analysis.²⁷ AFM measurements at $\text{pH} = 2$ and 8 (Figure S3) showed that the film remained homogeneous after swelling/deswelling and exhibited a minor increase in surface roughness from 3.4 to 4.6 nm (RMS).

Figure 3A presents the swelling and deswelling of the $B_{66}V_{34}^{126}$ film in water when switching the pH value between 2 and 8, as studied by *in situ* spectroscopic ellipsometry. The change in layer thickness and water uptake were evaluated using an effective medium model (for details see Supporting Information, Figure S4). At the initial pH of 8, the film exhibited a thickness of 162 nm with a water content of 40%. Upon switching to $\text{pH} = 2$, the pyridine units become water-soluble due to protonation, resulting in an increase in thickness to 329 nm. The additional swelling corresponds to a water content of 78%. Upon successive switching between low and

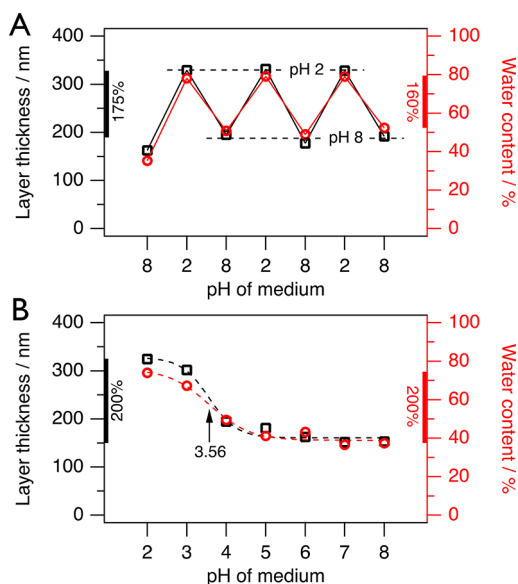


Figure 3. pH-responsive swelling/deswelling of a thin $B_{66}V_{34}^{126}$ film studied by *in situ* spectroscopic ellipsometry. (A) Reversible swelling and deswelling at pH = 2 and 8, respectively, over 3 cycles. (B) Layer thickness and water content in dependence of pH upon gradual transition from low to high pH.

high pH, the reversible swelling/deswelling was monitored over three cycles. As the direct transition from low to high pH is accompanied by a fast quenching of the polymer film, the film does not fully recover to its initial thickness. After cycle 1, the relative change in film thickness was 175%, which corresponds to a relative change in water content of 160% upon swelling. To study the pH-responsiveness in detail, the transition was monitored for incremental changes in pH (Figure 3B). Here, the polymer film fully returned to its initial thickness before pH cycling. The point of inflection was determined at a pH of 3.6, which is lower than the expected pK_a value for P2VP ($pK_a = 4.9$).^{25,26} This might be due to the nonpolar PB block, which leads to a decrease in pH at which significant swelling is observed. The maximum degree of swelling was 200%, which is consistent with an increase in water content by a factor of 2.

Immobilization of *C. glutamicum*. *C. glutamicum* was immobilized in PVA particles to ensure survivability throughout the electrospinning process from organic solvents. The successfully obtained PVA/bacteria hybrid particles are shown in Figure 4A and have an average diameter of $D = 5.9 \pm 3.1 \mu\text{m}$, as determined by SEM image analysis. The successful encapsulation of *C. glutamicum* was proven by placing the

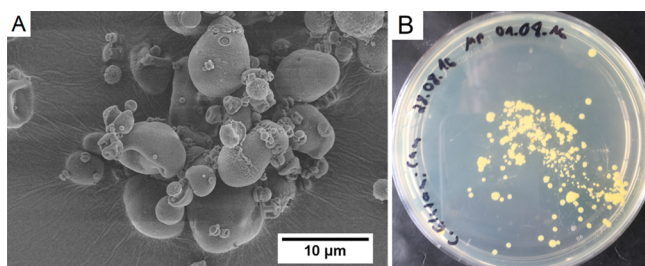


Figure 4. SEM image (A) of PVA/bacteria hybrid particles. (B) Digital photograph of *C. glutamicum* growth on an agar plate out of PVA particles.

PVA/bacteria hybrid particles on an agar plate and monitoring the bacterial out-growth, which revealed that living bacteria are inside these particles (Figure 4B).

To further confirm the presence of bacteria inside the PVA particles, confocal Raman imaging was used (Figure 5). The

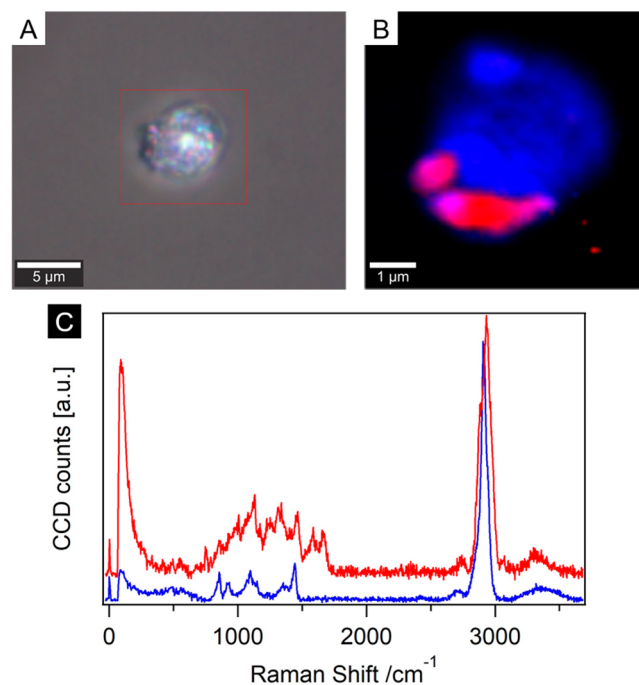


Figure 5. (A) Optical microscopy image of a PVA/bacteria hybrid particle indicating the position for Raman imaging (red box). (B) Raman cross section of the bacteria loaded PVA particle showing the spatial distribution of PVA (colored in blue) and *C. glutamicum* (colored in red). (C) Raman spectra of neat *C. glutamicum* (colored in red) and PVA (blue) used for Raman imaging analysis.

Raman cross section of the PVA/bacteria hybrid particle (corresponding optical microscopy image in Figure 5A) is given in Figure 5B and clearly shows the presence of *C. glutamicum* (colored in red), which are embedded within the PVA matrix (colored in blue). The respective Raman spectra of the neat components, PVA and *C. glutamicum*, which were used for Raman imaging analysis are depicted in Figure 5C.

Immobilization of *C. glutamicum* in Electrospun Fibers with a pH-Responsive Shell Using Coaxial Electrospinning. Employing coaxial electrospinning a special fiber morphology was obtained. The PB-*b*-P2VP diblock copolymer was used as the outer shell and a THF dispersion of PVA/bacteria particles was used as inner core within the coaxial electrospinning process (Scheme 1). The PB-*b*-P2VP diblock copolymer shell provides pH-responsiveness for further protection of the bacteria inside the PVA particles as well as mechanical stability in solution through subsequent cross-linking of the PB phase.

Figure 6A,B shows SEM images of an as-prepared nonwoven after cross-linking. It can be clearly seen that the PVA/bacteria hybrid particles are embedded within the PB-*b*-P2VP fibers, which build up the continuous nonwoven. An efficient encapsulation of the bacteria within the nonwovens is indispensable to avoid an additional contamination of OMW during phenol degradation. This was proven by incubating the nonwoven in growth media for 7 days at 30 $^{\circ}\text{C}$. No growth of

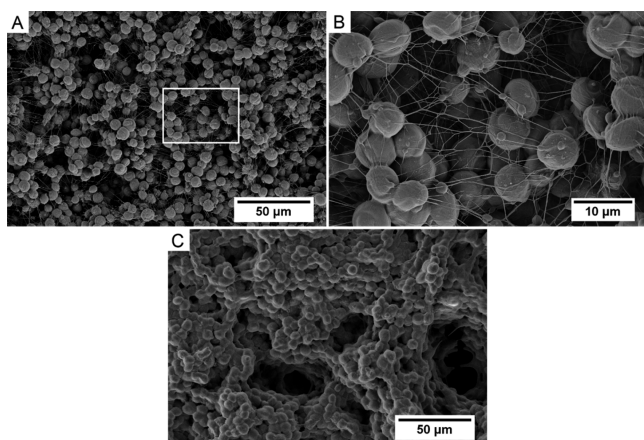


Figure 6. (A) SEM image of a nonwoven prepared by coaxial electrospinning with PVA/bacteria hybrid particles as the core and PB-*b*-P2VP as the outer shell, (B) shows the magnification of the area depicted by a white box in part A. (C) SEM image of the nonwoven after immersion in water of pH = 4 for 7 days.

bacteria could be observed after streaking the incubation media on an agar plate (Figure S5). Further methods for the quantification of bacteria inside the fiber mat could not be used, because common staining methods are influenced by the matrix and extraction is not possible due to the performed cross-linking. Therefore, the viability of bacteria could only be shown with the biodegradation of phenol, which is discussed later. As mentioned before, OMW is characterized by low pH values down to pH = 4. Therefore, stability of the materials in such environments is indispensable. For testing, the nonwoven with embedded PVA/bacteria hybrid particles was immersed in a solution of pH = 4 for 7 days. The nonwoven stayed stable for the complete time period. However, due to the swelling of the outer PB-*b*-P2VP diblock copolymer shell at low pH the structure of the nonwoven changed. The small fibers in between the PVA/bacteria particles are not observable anymore and the particles themselves are more densely packed (Figure 6C).

Phenol Degradation by Planktonic Cells of *C. glutamicum* at Different pH. The viability and phenol degradation capacity of *C. glutamicum* was analyzed using planktonic cells in minimal medium at different pH values, applying a phenol concentration of $c = 0.4 \text{ g L}^{-1}$. At pH values of 4 and 5 (Figure 7A,B), the growth of *C. glutamicum* was inhibited completely, in contrast to the observed growth and biological activity (phenol degradation) at neutral pH (Figure 7C,D). As shown in Figure 7B, no colonies were observed after streaking the *C. glutamicum* solutions of pH = 4 and pH = 5 onto agar plates, which indicates no viability of these bacteria under acidic conditions. This is in-line with the reported low tolerance of phenol degrading microorganisms of *Acinetobacter* species to acidic conditions.²⁸ Therefore, phenol degradation at low pH was not possible, which clearly shows the necessity of protecting *C. glutamicum* for use in purification of OMW which has a pH value as low as pH = 4.

Figure 7C shows the correlation between bacteria growth and phenol degradation at pH = 7. In contrast to the results at lower pH, planktonic cells degraded the initial phenol content below the detection limit within a time period of 5 days. In addition, bacteria remained viable during the stationary phase, where no further bacteria growth was observed (incubation time >1 day), as indicated by the continuing phenol

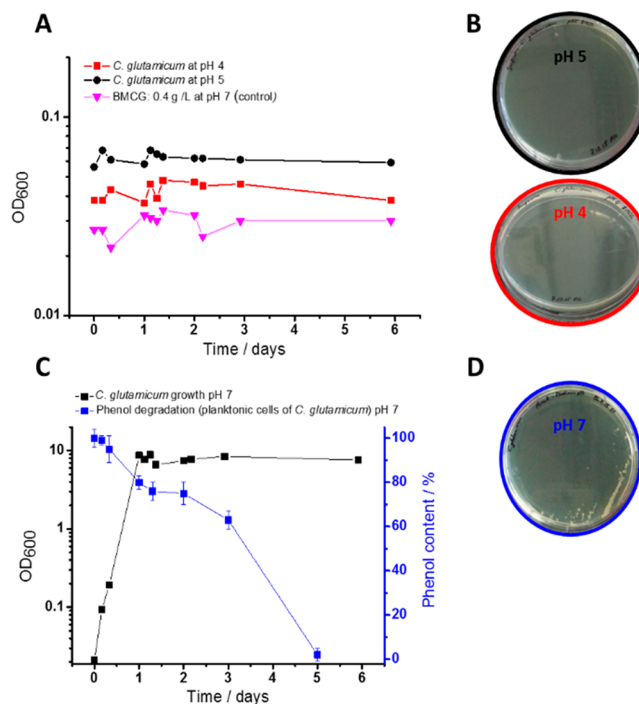


Figure 7. (A) Growth study of *C. glutamicum* at pH = 4 and 5 and a control group without bacteria in minimal media with a phenol concentration of $c = 0.4 \text{ g L}^{-1}$ at $30 \text{ }^{\circ}\text{C}$, all samples show no growth of bacteria. (B) No growth of *C. glutamicum* was observed on agar plates after streaking from acidic solution (72 h at $30 \text{ }^{\circ}\text{C}$). (C) *C. glutamicum* growth and phenol degradation at pH = 7. (D) Growth of *C. glutamicum* on an agar plate after streaking from neutral solution (72 h at $30 \text{ }^{\circ}\text{C}$).

degradation. Moreover, the growth of *C. glutamicum* on agar plates after phenol degradation in minimal media confirmed the viability of these microorganisms under the applied conditions (Figure 7D).

Phenol Degradation by Immobilized *C. glutamicum* at Different pH. First, we studied phenol degradation with PVA/bacteria hybrid particles at pH = 7 to probe the effect of encapsulation on the phenol degradation efficiency of *C. glutamicum* (Figure 8A). For all degradation studies a phenol concentration of $c = 0.4 \text{ g L}^{-1}$ was used. At pH = 7 degradation of around 30% was achieved by the PVA encapsulated bacteria within 48 h, employing 20 mg of the particles. This shows that the encapsulated bacteria are still active in phenol degradation and in turn can be employed in coaxial electrospinning from organic solvents to produce the desired pH-responsive PB-*b*-P2VP nonwovens with embedded PVA/bacteria particles that allow phenol degradation in a medium with a low pH of 4 such as in OMW. Figure 8B shows that with bacteria loaded PB-*b*-P2VP nonwovens at pH = 4 and 7 about 9 and 12% of the phenol were degraded after 2 days, respectively. After that degradation practically stopped. These results show that phenol degradation at pH = 4 is possible with the biohybrid PB-*b*-P2VP nonwovens and that the concept of protecting the embedded bacteria with a pH-responsive block copolymer is successful. An influence of the PB-*b*-P2VP based nonwoven can be ruled out, as a corresponding blank experiment without encapsulated bacteria showed no effect on phenol concentration (Figure S6)

We carried out an additional systematic study of a “dose-response curve” by changing the size of the nonwovens used

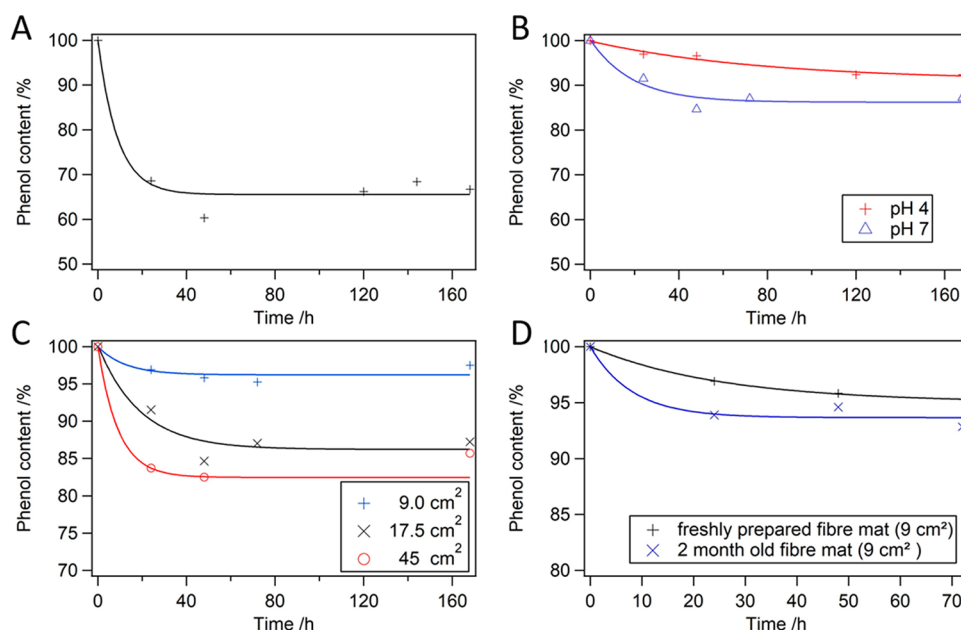


Figure 8. (A) Degradation of phenol with neat PVA/bacteria hybrid particles at pH = 7 (amount of PVA/bacteria particles: 20 mg). Comparison of phenol degradation with PVA/bacteria particles encapsulated in PB-b-P2VP nonwovens: (B) at pH = 4 (size, 14 cm²) and pH = 7 (size, 17.5 cm²), (C) for different sizes of the employed nonwovens at pH = 7, and (D) comparison of a freshly prepared and stored (for 2 months at 4 °C) nonwoven at pH = 7. The degradation studies were performed for at least 7 days in minimal media employing a phenol concentration of $c = 0.4 \text{ g L}^{-1}$ at 30 °C. A blank test is shown in Figure S6.

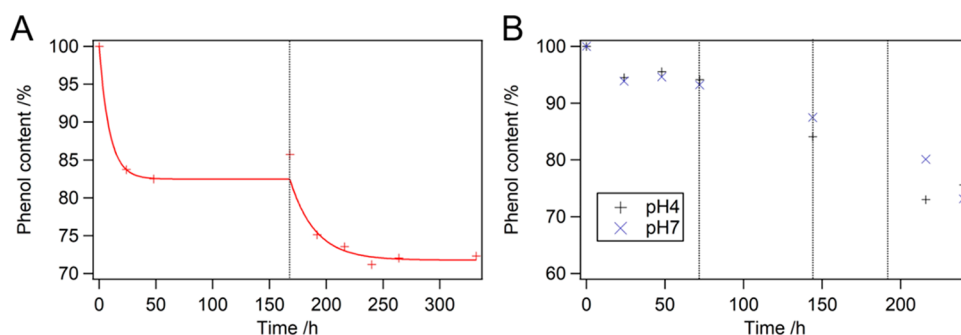


Figure 9. (A) Stepwise degradation of phenol at pH = 7 with addition of glucose after 168 h (sample size, 45 cm²). (B) Phenol degradation upon continuous addition of glucose at pH = 4 and 7 (sample size, 9 cm²; addition of glucose is indicated by dotted lines).

and thereby also the amount of biocatalyst present in the system. A semiquantitative comparison of the degradation efficiency of encapsulated bacteria and bacteria loaded nonwovens is possible, as all nonwovens contained approximately 4.5 mg of PVA/bacteria particles per 10 cm². Thus, the influence of the amount of bacteria on phenol degradation can be probed by varying the size of the employed nonwovens and can be further compared to the degradation study with neat PVA/bacteria particles. In fact, with increasing size a significant increase in phenol degradation was observed (Figure 8C). For the largest nonwoven with a size of 45 cm², which corresponds to an amount of encapsulated bacteria of about 20 mg, a phenol degradation of 20% could be reached at pH = 7. This is 10% less with respect to the phenol degradation of 30% reached with a comparable amount of neat PVA/bacteria particles. However, it can also be seen that degradation was only observable within the first 72 h and then practically stopped, an issue that will be addressed later on.

Another important issue with respect to application of bioactive nonwovens for phenol degradation is their suitability for storage. Hence, it was tested if the degradation potential is

influenced by the storage of nonwovens for 2 months. To decrease the influence of inhomogeneities, parts of the same nonwovens were used in these experiments. Figure 8D shows that the reached phenol degradation was almost the same for both the freshly prepared and the 2-month-old nonwoven (around 5%) at pH = 7. This indicates that the nonwovens are storable for some time and that the bacteria remain alive and metabolically active inside the nonwoven. The observed small differences are well within the expected experimental error due to thickness variations within the nonwoven, i.e., slightly different amounts of bacteria within the nonwoven samples.

Free *C. glutamicum* is known to require a second carbon source for the efficient degradation of phenol.^{22,29} Consequently, we hypothesized that a possible reason for the limited phenol degradation observed by us when using bacteria immobilized in nonwovens might be a depletion in the glucose concentration during degradation. Indeed, through the simple addition of some glucose after the first degradation step, it was possible to restart the degradation and achieve a degradation of around 30% at pH = 7 (Figure 9A), which is comparable to the value obtained for the PVA/bacteria particles (Figure 8A).

Bacteria therefore survive inside the nonwoven during this period and can be reactivated through the addition of glucose. Moreover, a similar result can be achieved by a continuous addition of glucose, resulting in an overall degradation of around 30% even at pH = 4 (Figure 9B).

CONCLUSION

Successful immobilization of *C. glutamicum* as an active agent for phenol degradation in an elastic and pH-responsive nonwoven, employing a two-step process based on coaxial electrospinning, was shown. This effectively protects the embedded bacteria from the otherwise toxic low pH values of olive mill wastewater, enabling a direct use of these tea-bag like biohybrid systems for phenol degradation at low pH. With this system it is possible to reach a phenol degradation of about 30% at pH = 4 (initial phenol concentration of $c = 0.4 \text{ g L}^{-1}$, $30 \text{ }^\circ\text{C}$), whereas no degradation was observed for planktonic cells under similar conditions, as they do not survive at such a low pH. Bacteria could be reactivated for phenol degradation by addition of a second carbon source. The biohybrid system with immobilized bacteria is storable (at least 2 months as studied in this work) with bacteria remaining alive and metabolically active for phenol degradation. A comparison with planktonic cells at pH = 7 revealed that the two-step encapsulation of the bacteria in the nonwoven limits the achievable phenol degradation to about 30%, whereas the free bacteria are able to completely degrade the supplied phenol. The origin of this confinement effect and the optimization of the encapsulation process to yield higher degradation rates even at low pH will be the focus of future studies.

This concept of combining a pH-responsive diblock copolymer with coaxial electrospinning of PVA/bacteria particles provides a versatile method for a variety of materials and applications, especially as biocarrier or catalytic platform. The encapsulation of the bacteria particles in a protecting elastic matrix creates a microenvironment in which the bacteria are protected even against harsh conditions, which would otherwise kill the bacteria. This significantly expands the use of bacteria for the degradation of pollutants in wastewater.

ASSOCIATED CONTENT

Supporting Information

The Supporting Information is available free of charge on the ACS Publications website at DOI: 10.1021/acs.biomac.8b00361.

Detailed synthetical procedure and characterization of the PB-*b*-P2VP diblock copolymer, mechanical properties of PB-*b*-P2VP films and fibers, AFM studies on polymeric films for swelling behavior, ellipsometric study on swelling behavior, and determination of *C. glutamicum* leakage from PB-*b*-P2VP electrospun fibers (PDF)

AUTHOR INFORMATION

Corresponding Author

*E-mail: agarwal@uni-bayreuth.de.

ORCID

Christian Kuttner: 0000-0002-4093-7469

Ruth Freitag: 0000-0003-4642-897X

Seema Agarwal: 0000-0002-3174-3152

Author Contributions

‡M.P. and B.A.P.-C. contributed equally to this work.

Notes

The authors declare no competing financial interest.

ACKNOWLEDGMENTS

The authors are indebted to the Deutsche Forschungsgemeinschaft (DFG; GIP Project) and BayBioTec for financial support. C.K. acknowledges funding from the European Union's Horizon 2020 research and innovation program under the Marie Skłodowska-Curie Grant Agreement No. 799393 (NANOBIOME). In addition, we would like to thank Paul Pineda Contreras, Markus Langner, and Matthias Burgard for providing important analytical support to this work.

ABBREVIATIONS

AFM, atomic force microscopy; CFU, colony forming units; *C. glutamicum*, *Corynebacterium glutamicum*; CQ, campherquione; DCTB, (*trans*-2-[3-(4-*tert*-butylphenyl)-2-methyl-2-propenylidene]malononitrile); EDMAB, ethyl 4-(dimethylamino)benzoate; Et₃Al, triethylaluminum; OMW, olive oil mill wastewater; PB-*b*-P2VP, polybutadiene-*block*-poly(2-vinylpyridine); PVA, poly(vinyl alcohol); *sec*-BuLi, *sec*-butyllithium; SEC, size exclusion chromatography; TEM, transmission electron microscopy; SEM, scanning electron microscopy

REFERENCES

- (1) Krastanov, A.; Alexieva, Z.; Yemendzhiev, H. Microbial degradation of phenol and phenolic derivatives. *Eng. Life Sci.* **2013**, *13*, 76–87.
- (2) Zhu, X.; Tian, J.; Chen, L. Phenol degradation by isolated bacterial strains: kinetics study and application in coking wastewater treatment. *J. Chem. Technol. Biotechnol.* **2012**, *87*, 123–129.
- (3) Heilbuth, N. M.; Linardi, V. R.; Monteiro, A. S.; da Rocha, R. A.; Mimim, L. A.; Santos, V. L. Estimation of kinetic parameters of phenol degradation by bacteria isolated from activated sludge using a genetic algorithm. *J. Chem. Technol. Biotechnol.* **2015**, *90*, 2066–2075.
- (4) La Cara, F.; Ionata, E.; Del Monaco, G.; Marcolongo, L.; Gonçalves, M. R.; Marques, I. P. Olive mill wastewater anaerobically digested: Phenolic compounds with antiradical activity. *Chem. Eng. Trans.* **2012**, *27*, 325–330.
- (5) Paraskeva, P.; Diamadopoulos, E. Technologies for olive mill wastewater (OMW) treatment: a review. *J. Chem. Technol. Biotechnol.* **2006**, *81*, 1475–1485.
- (6) Azaizeh, H.; Jadoun, J. Co-digestion Of Olive Mill Wastewater and Swine Manure Using Up-Flow Anaerobic Sludge Blanket Reactor for Biogas Production. *J. Water Resour. Prot.* **2010**, *2*, 314–321.
- (7) Morillo, J. A.; Antizar-Ladislao, B.; Monteoliva-Sánchez, M.; Ramos-Cormenzana, A.; Russell, N. J. Bioremediation and biovalorisation of olive-mill wastes. *Appl. Microbiol. Biotechnol.* **2009**, *82*, 25–39.
- (8) Mantzavinos, D.; Kalogerakis, N. Treatment of olive mill effluents: Part I. Organic matter degradation by chemical and biological processes—an overview. *Environ. Int.* **2005**, *31*, 289–295.
- (9) Leonard, D.; Lindley, N. D. Carbon and energy flux constraints in continuous cultures of *Alcaligenes eutrophus* grown on phenol. *Microbiology* **1998**, *144*, 241–248.
- (10) Geng, A.; Soh, A. E. W.; Lim, C. J.; Loke, L. C. T. Isolation and characterization of a phenol-degrading bacterium from an industrial activated sludge. *Appl. Microbiol. Biotechnol.* **2006**, *71*, 728–735.
- (11) Dhoub, A.; Aloui, F.; Hamad, N.; Sayadi, S. Pilot-plant treatment of olive mill wastewaters by *Phanerochaete chrysosporium* coupled to anaerobic digestion and ultrafiltration Process. *Process Biochem.* **2006**, *41*, 159–167.

(12) Zahid, M. S. B.; Iqbal, A.; Arshad, M. Benzene degradation with bacterial strains isolated from rhizosphere of *Cannabis sativa* being irrigated with petroleum refinery wastewater. *Desalin. Water Treat.* **2016**, *57*, 17579–17584.

(13) Sivaprakasam, S.; Mahadevan, S.; Sekar, S.; Rajakumar. Biological treatment of tannery wastewater by using salt-tolerant bacterial strains. *Microb. Cell Fact.* **2008**, *7*, 15.

(14) Alam, M. Z.; Muyibi, S. A.; Jamal, P. Biological treatment of sewage treatment plant sludge by pure bacterial culture with optimum process conditions in a stirred tank bioreactor. *J. Environ. Sci. Health, Part A: Toxic/Hazard. Subst. Environ. Eng.* **2007**, *42*, 1671–1679.

(15) Le, T.-H.; Kim, S. J.; Bang, S. H.; Lee, S.-H.; Choi, Y. W.; Kim, P.; Kim, Y.-H. Min, Degradation and assimilation of aromatic compounds by *Corynebacterium glutamicum*: another potential for applications for this bacterium? *Bioresour. Technol.* **2012**, *104*, 795–798.

(16) Shen, X.-H.; Zhou, N.-Y.; Liu, S.-J. Degradation and assimilation of aromatic compounds by *Corynebacterium glutamicum*: Another potential for applications for this bacterium? *Appl. Microbiol. Biotechnol.* **2012**, *95*, 77–89.

(17) Pishgar, R.; Najafpour, G.; Neyra, B. N.; Mousavi, N.; Bakhshi, Z. Anaerobic Biodegradation of Phenol: Comparative Study of Free and Immobilized Growth. *Iran. J. Energy Environ.* **2011**, *2*, 348–355.

(18) Greiner, A.; Wendorff, J. H. Electrospinning: a fascinating method for the preparation of ultrathin fibers. *Angew. Chem., Int. Ed.* **2007**, *46*, 5670–5703.

(19) Gensheimer, M.; Brandis-Heep, A.; Agarwal, S.; Thauer, R. K.; Greiner, A. Polymer/bacteria composite nanofiber nonwovens by electrospinning of living bacteria protected by hydrogel micro-particles. *Macromol. Biosci.* **2011**, *11*, 333–337.

(20) Knierim, Ch.; Enzeroth, M.; Kaiser, P.; Dams, Ch.; Nette, D.; Seubert, A.; Klingl, A.; Greenblatt Ch, L.; Jérôme, V.; Agarwal, S.; Freitag, R.; Greiner, A. Living composites of bacteria and polymers as biomimetic biofilms for metal sequestration and bioremediation. *Macromol. Biosci.* **2015**, *15*, 1052–1059.

(21) Letnik, I.; Avrahami, R.; Rokem, J. S.; Greiner, A.; Zussman, E.; Greenblatt, Ch. L. Living composites of electrospun yeast cells for bioremediation and ethanol production. *Biomacromolecules* **2015**, *16*, 3322–3328.

(22) Nardi, A.; Avrahami, R.; Zussman, E.; Rokem, J. S.; Greenblatt, C. L. Phenol Biodegradation by *Corynebacterium glutamicum* Encapsulated in Electrospun Fibers. *J. Environ. Prot.* **2012**, *3*, 164–168.

(23) Liebl, W.; Klamer, R.; Schleifer, K. H. Requirement of chelating compounds for the growth of *Corynebacterium glutamicum* in synthetic media. *Appl. Microbiol. Biotechnol.* **1989**, *32*, 205–210.

(24) Walther, A.; Goldmann, A. S.; Yelamanchili, R. S.; Drechsler, M.; Schmalz, H.; Eisenberg, A.; Müller, A. H. E. Multiple Morphologies, Phase Transitions, and Cross-Linking of Crew-Cut Aggregates of Polybutadiene-block-poly(2-vinylpyridine) Diblock Copolymers. *Macromolecules* **2008**, *41*, 3254–3260.

(25) Dupin, D.; Fujii, S.; Armes, S. P.; Hill, B.; Reeve, S. P.; Reeve, P.; Baxter, S. M. Efficient synthesis of sterically stabilized pH-responsive microgels of controllable particle diameter by emulsion polymerization. *Langmuir* **2006**, *22*, 3381–3387.

(26) Reinicke, S.; Schmelz, J.; Lapp, A.; Karg, M.; Hellweg, T.; Schmalz, H. Smart hydrogels based on double responsive triblock terpolymers. *Soft Matter* **2009**, *5*, 2648–2657.

(27) Kuttner, C.; Hanisch, A.; Schmalz, H.; Eder, M.; Schlaad, H.; Burgert, I.; Fery, A. Influence of the Polymeric Interphase Design on the Interfacial Properties of (Fiber-Reinforced) Composites. *ACS Appl. Mater. Interfaces* **2013**, *5*, 2469–2478.

(28) Wang, Y.; Tian, Y.; Han, B.; Zhao, H.-B.; Bi, J.-N.; Cai, B.-L. Biodegradation of phenol by free and immobilize. *Acinetobacter* sp. strain PD12. *J. Environ. Sci.* **2007**, *19*, 222–225.

(29) Qi, S.-W.; Chaudhry, M. T.; Zhang, Y.; Meng, B.; Huang, Y.; Zhao, K.-X.; Poetsch, A.; Jiang, C.-Y.; Liu, S.; Liu, S. J. Comparative proteomes of *Corynebacterium glutamicum* grown on aromatic compounds revealed novel proteins involved in aromatic degradation

and a clear link between aromatic catabolism and gluconeogenesis via fructose-1,6-bisphosphatase. *Proteomics* **2007**, *7*, 3775–3787.